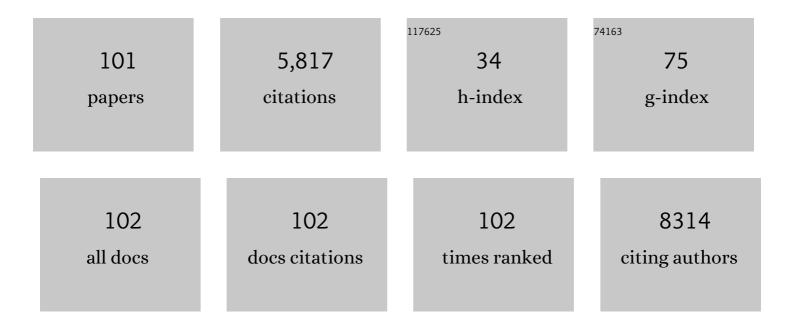
List of Publications by Year in descending order

Source: https://exaly.com/author-pdf/698161/publications.pdf Version: 2024-02-01



XIAO LINI

#	Article	IF	CITATIONS
1	Electromagnetic Interference (EMI) Shielding of Single-Walled Carbon Nanotube Epoxy Composites. Nano Letters, 2006, 6, 1141-1145.	9.1	1,106
2	Commensurate–incommensurate transition in graphene on hexagonal boron nitride. Nature Physics, 2014, 10, 451-456.	16.7	737
3	The influence of single-walled carbon nanotube structure on the electromagnetic interference shielding efficiency of its epoxy composites. Carbon, 2007, 45, 1614-1621.	10.3	524
4	Microwave Absorption of Single-Walled Carbon Nanotubes/Soluble Cross-Linked Polyurethane Composites. Journal of Physical Chemistry C, 2007, 111, 13696-13700.	3.1	324
5	Site-Specific Kondo Effect at Ambient Temperatures in Iron-Based Molecules. Physical Review Letters, 2007, 99, 106402.	7.8	242
6	Intrinsically patterned two-dimensional materials for selective adsorption of molecules andÂnanoclusters. Nature Materials, 2017, 16, 717-721.	27.5	150
7	Recent progress in degradation and stabilization of organic solar cells. Journal of Power Sources, 2014, 264, 168-183.	7.8	136
8	Quantum Well States in Two-Dimensional Gold Clusters on MgO Thin Films. Physical Review Letters, 2009, 102, 206801.	7.8	128
9	Epitaxial Growth of Iron Phthalocyanine at the Initial Stage on Au(111) Surface. Journal of Physical Chemistry C, 2007, 111, 2656-2660.	3.1	124
10	Charge-Mediated Adsorption Behavior of CO on MgO-Supported Au Clusters. Journal of the American Chemical Society, 2010, 132, 7745-7749.	13.7	112
11	Epitaxial Growth of Honeycomb Monolayer CuSe with Dirac Nodal Line Fermions. Advanced Materials, 2018, 30, e1707055.	21.0	110
12	Epitaxial growth and physical properties of 2D materials beyond graphene: from monatomic materials to binary compounds. Chemical Society Reviews, 2018, 47, 6073-6100.	38.1	97
13	Construction of 2D Atomic Crystals on Transition Metal Surfaces: Graphene, Silicene, and Hafnene. Small, 2014, 10, 2215-2225.	10.0	91
14	Construction of bilayer PdSe2 on epitaxial graphene. Nano Research, 2018, 11, 5858-5865.	10.4	84
15	Direct visualization of atomically precise nitrogen-doped graphene nanoribbons. Applied Physics Letters, 2014, 105, .	3.3	82
16	Stable, Reproducible Nanorecording on Rotaxane Thin Films. Journal of the American Chemical Society, 2005, 127, 15338-15339.	13.7	77
17	Gas transport in porous electrodes of solid oxide fuel cells: A review on diffusion and diffusivity measurement. Journal of Power Sources, 2013, 237, 64-73.	7.8	73
18	Intrinsic current-voltage properties of nanowires with four-probe scanning tunneling microscopy: A conductance transition of ZnO nanowire. Applied Physics Letters, 2006, 89, 043103.	3.3	72

#	Article	IF	CITATIONS
19	Characterizing low-coordinated atoms at the periphery of MgO-supported Au islands using scanning tunneling microscopy and electronic structure calculations. Physical Review B, 2010, 81, .	3.2	67
20	Charge-induced formation of linear Au clusters on thin MgO films: Scanning tunneling microscopy and density-functional theory study. Physical Review B, 2008, 78, .	3.2	64
21	Structure and Dynamics of CO ₂ on Rutile TiO ₂ (110)-1×1. Journal of Physical Chemistry C, 2012, 116, 26322-26334.	3.1	60
22	Localized spin-orbit polaron in magnetic Weyl semimetal Co3Sn2S2. Nature Communications, 2020, 11, 5613.	12.8	53
23	Role of Lateral Alkyl Chains in Modulation of Molecular Structures on Metal Surfaces. Physical Review Letters, 2006, 96, 226101.	7.8	51
24	Identifying and Visualizing the Edge Terminations of Single-Layer MoSe ₂ Island Epitaxially Grown on Au(111). ACS Nano, 2017, 11, 1689-1695.	14.6	48
25	5f Covalency Synergistically Boosting Oxygen Evolution of UCoO ₄ Catalyst. Journal of the American Chemical Society, 2022, 144, 416-423.	13.7	48
26	Dimerization Induced Deprotonation of Water on RuO ₂ (110). Journal of Physical Chemistry Letters, 2014, 5, 3445-3450.	4.6	47
27	Selective Analysis of Molecular States by Functionalized Scanning Tunneling Microscopy Tips. Physical Review Letters, 2006, 96, 156102.	7.8	44
28	Sulfur-doped graphene nanoribbons with a sequence of distinct band gaps. Nano Research, 2017, 10, 3377-3384.	10.4	44
29	Uniform Doping of Titanium in Hematite Nanorods for Efficient Photoelectrochemical Water Splitting. ACS Applied Materials & Interfaces, 2015, 7, 14072-14078.	8.0	43
30	Direct growth of wafer-scale highly oriented graphene on sapphire. Science Advances, 2021, 7, eabk0115.	10.3	43
31	Spontaneous Formation of 1D Pattern in Monolayer VSe ₂ with Dispersive Adsorption of Pt Atoms for HER Catalysis. Nano Letters, 2019, 19, 4897-4903.	9.1	42
32	Nucleation and Growth of Gold on MgO Thin Films:  A Combined STM and Luminescence Study. Journal of Physical Chemistry C, 2007, 111, 10528-10533.	3.1	39
33	High quality PdTe2 thin films grown by molecular beam epitaxy. Chinese Physics B, 2018, 27, 086804.	1.4	39
34	Observation of Structural and Conductance Transition of Rotaxane Molecules at a Submolecular Scale. Advanced Functional Materials, 2007, 17, 770-776.	14.9	37
35	Self-Assembly of MgPc Molecules on Polar FeO Thin Films. Journal of Physical Chemistry C, 2008, 112, 15325-15328.	3.1	34
36	Construction of Two-Dimensional Chiral Networks through Atomic Bromine on Surfaces. Journal of Physical Chemistry Letters, 2017, 8, 326-331.	4.6	33

Χίαο Lin

#	Article	IF	CITATIONS
37	Site- and Configuration-Selective Anchoring of Iron–Phthalocyanine on the Step Edges of Au(111) Surface. Journal of Physical Chemistry C, 2011, 115, 10791-10796.	3.1	31
38	Understanding and controlling the weakly interacting interface inperyleneâ^•Ag(110). Physical Review B, 2006, 73, .	3.2	29
39	Crystalline Thin Films Formed by Supramolecular Assembly for Ultrahigh-Density Data Storage. Advanced Materials, 2004, 16, 2018-2021.	21.0	27
40	Surface reconstruction transition of metals induced by molecular adsorption. Physical Review B, 2011, 83, .	3.2	26
41	Airâ€Stable Monolayer Cu ₂ Se Exhibits a Purely Thermal Structural Phase Transition. Advanced Materials, 2020, 32, e1908314.	21.0	26
42	Sizable Band Gap in Epitaxial Bilayer Graphene Induced by Silicene Intercalation. Nano Letters, 2020, 20, 2674-2680.	9.1	23
43	CO Adsorption on Thin MgO Films and Single Au Adatoms: A Scanning Tunneling Microscopy Study. Journal of Physical Chemistry C, 2010, 114, 8997-9001.	3.1	22
44	The evaluation of Coulombic interaction in the oriented-attachment growth of colloidal nanorods. Analyst, The, 2012, 137, 4917.	3.5	21
45	Modification of the Potential Landscape of Molecular Rotors on Au(111) by the Presence of an STM Tip. Nano Letters, 2018, 18, 4704-4709.	9.1	21
46	Surface crystallization effects on the optical and electric properties of CdS nanorods. Nanotechnology, 2005, 16, 2402-2406.	2.6	20
47	Site-Specific Imaging of Elemental Steps in Dehydration of Diols on TiO ₂ (110). ACS Nano, 2013, 7, 10414-10423.	14.6	20
48	Tuning the morphology of chevron-type graphene nanoribbons by choice of annealing temperature. Nano Research, 2018, 11, 6190-6196.	10.4	20
49	An electrochemical device for three-dimensional (3D) diffusivity measurement in fuel cells. Nano Energy, 2013, 2, 1004-1009.	16.0	19
50	Insulating SiO ₂ under Centimeter-Scale, Single-Crystal Graphene Enables Electronic-Device Fabrication. Nano Letters, 2020, 20, 8584-8591.	9.1	19
51	Structural evolution at the initial growth stage of perylene on Au(111). Surface Science, 2007, 601, 3179-3185.	1.9	17
52	Stabilizing Cold Adatoms by Thiophenyl Derivatives: A Possible Route toward Metal Redispersion. Journal of the American Chemical Society, 2012, 134, 11161-11167.	13.7	16
53	OH Group Dynamics of 1,3-Propanediol on TiO2(110). Journal of Physical Chemistry Letters, 2012, 3, 3257-3263.	4.6	16
54	Force-Activated Isomerization of a Single Molecule. Journal of the American Chemical Society, 2020, 142, 10673-10680.	13.7	16

#	Article	IF	CITATIONS
55	Two distinct superconducting states controlled by orientations of local wrinkles in LiFeAs. Nature Communications, 2021, 12, 6312.	12.8	16
56	Direct observation of surface structure of d-alanine and d-/l-valine crystals by atomic force microscopy and comparison with X-ray diffraction analysis. Surface Science, 2002, 512, L379-L384.	1.9	15
57	Interaction of CO2 with oxygen adatoms on rutile TiO2(110). Physical Chemistry Chemical Physics, 2013, 15, 6190.	2.8	13
58	Construction of single-crystalline supramolecular networks of perchlorinated hexa- <i>peri</i> -hexabenzocoronene on Au(111). Journal of Chemical Physics, 2015, 142, 101911.	3.0	13
59	Honeycomb AgSe Monolayer Nanosheets for Studying Two-dimensional Dirac Nodal Line Fermions. ACS Applied Nano Materials, 2021, 4, 8845-8850.	5.0	13
60	Quantitative evaluation of Coulombic interactions in the oriented-attachment growth of nanotubes. Analyst, The, 2014, 139, 371-374.	3.5	12
61	Layer-by-Layer Epitaxy of Porphyrinâ^Ligand Fe(II)-Fe(III) Nanoarchitectures for Advanced Metal–Organic Framework Growth. ACS Applied Nano Materials, 2020, 3, 11752-11759.	5.0	12
62	Chirality locking charge density waves in a chiral crystal. Nature Communications, 2022, 13, .	12.8	12
63	Manipulation and four-probe analysis of nanowires in UHV by application of four tunneling microscope tips: a new method for the investigation of electrical transport through nanowires. Surface and Interface Analysis, 2006, 38, 1096-1102.	1.8	11
64	Centimeter-scale, single-crystalline, AB-stacked bilayer graphene on insulating substrates. 2D Materials, 2019, 6, 045044.	4.4	11
65	Unexpected Roles of Alkali-Metal Cations in the Assembly of Low-Valent Uranium Sulfate Molecular Complexes. Inorganic Chemistry, 2020, 59, 2348-2357.	4.0	11
66	Recovery of edge states of graphene nanoislands on an iridium substrate by silicon intercalation. Nano Research, 2018, 11, 3722-3729.	10.4	10
67	Experimental Synthesis of Strained Monolayer Silver Arsenide on Ag(111) Substrates. Chinese Physics Letters, 2020, 37, 068103.	3.3	10
68	Three-dimensional microstructural characterization of solid oxide electrolysis cell with CeO.8Gd0.2O2-infiltrated Ni/YSZ electrode using focused ion beam-scanning electron microscopy. Journal of Solid State Electrochemistry, 2021, 25, 1633-1644. Jonalayer combinate	2.5	10
69	xmlns:mml="http://www.w3.org/1998/Math/MathÁL" display="inline"> <mml:mrow><mml:msub><mml:mrow><mml:mi>TiSe</mml:mi></mml:mrow><mml:mrow><mi stretchy="false">(<mml:mn>1</mml:mn>111</mi </mml:mrow></mml:msub></mml:mrow>	nl:mn>2< j ETQq1 1	/mml:mn> /<br 0.784314 rg
70	2022, 128, 026401. Line defects in monolayer TiSe2 with adsorption of Pt atoms potentially enable excellent catalytic activity. Nano Research, 2022, 15, 4687-4692.	10.4	9
71	High quality sub-monolayer, monolayer, and bilayer graphene on Ru(0001). Chinese Physics B, 2014, 23, 098101.	1.4	8
72	Synthesis of palladium nanoparticles on TiO ₂ (110) using a beta-diketonate precursor. Physical Chemistry Chemical Physics, 2015, 17, 6470-6477.	2.8	7

#	Article	IF	CITATIONS
73	Edge- and strain-induced band bending in bilayer-monolayer Pb2Se3 heterostructures. Chinese Physics B, 2021, 30, 018105.	1.4	7
74	Intercalation of germanium oxide beneath large-area and high-quality epitaxial graphene on Ir(111) substrate*. Chinese Physics B, 2021, 30, 048102.	1.4	7
75	A Tunable Amorphous Heteronuclear Iron and Cobalt Imidazolate Framework Analogue for Efficient Oxygen Evolution Reactions. European Journal of Inorganic Chemistry, 2021, 2021, 702-707.	2.0	7
76	Epitaxial synthesis and electronic properties of monolayer Pd ₂ Se ₃ *. Chinese Physics B, 2020, 29, 098102.	1.4	7
77	Patterns formed on the dimer vacancy array of Si(100) by self-assembly. Nanotechnology, 2002, 13, 729-732.	2.6	6
78	Controllable Density of Atomic Bromine in a Two-Dimensional Hydrogen Bond Network. Journal of Physical Chemistry C, 2018, 122, 25681-25684.	3.1	6
79	Epitaxial fabrication of two-dimensional TiTe2 monolayer on Au(111) substrate with Te as buffer layer. Chinese Physics B, 2019, 28, 056801.	1.4	6
80	On-Surface Synthesis and Characterization of Polythiophene Chains. Journal of Physical Chemistry C, 2020, 124, 764-768.	3.1	6
81	The As-surface of an iron-based superconductor CaKFe4As4. Nano Research, 2021, 14, 3921-3925.	10.4	6
82	Electrochemical devices with optimized gas tightness for the diffusivity measurement in fuel cells. International Journal of Hydrogen Energy, 2014, 39, 2334-2339.	7.1	5
83	Epitaxial fabrication of monolayer copper arsenide on Cu(111)*. Chinese Physics B, 2020, 29, 077301.	1.4	5
84	Growth of LaCoO ₃ crystals in molten salt: effects of synthesis conditions. CrystEngComm, 2021, 23, 671-677.	2.6	5
85	MgO intercalation and crystallization between epitaxial graphene and Ru(0001). Rare Metals, 0, , 1.	7.1	5
86	Controllable fabrication and photocatalytic performance of nanoscale single-layer MoSe ₂ islands with substantial edges on an Ag(111) substrate. Nanoscale, 2021, 13, 19165-19171.	5.6	5
87	Se-concentration dependent superstructure transformations of CuSe monolayer on Cu(111) substrate. 2D Materials, 2022, 9, 015017.	4.4	5
88	Rational Design of Two-Layer Fe-Doped PrBa _{0.8} Ca _{0.2} Co ₂ O _{6â^´î^} Double Perovskite Oxides for High-Performance Fuel Cell Cathodes. Journal of Physical Chemistry C, 2021, 125, 26448-26459.	3.1	5
89	Effects of graphene defects on Co cluster nucleation and intercalation. Chinese Physics B, 2014, 23, 088108.	1.4	3
90	Coulombic interaction in the colloidal oriented-attachment growth of tetragonal nanorods. Chinese Physics B, 2014, 23, 056103.	1.4	3

#	Article	IF	CITATIONS
91	Study of the relationship between the local geometric structure and the stability of La0.6Sr0.4MnO3â^δ and La0.6Sr0.4FeO3â^δ electrodes. Nuclear Science and Techniques/Hewuli, 2019, 30, 1.	3.4	3
92	Novel two-dimensional transition metal chalcogenides created by epitaxial growth. Science China: Physics, Mechanics and Astronomy, 2021, 64, 1.	5.1	3
93	Intrinsically Honeycombâ€Patterned Hydrogenated Graphene. Small, 2022, 18, e2102687.	10.0	3
94	Intrinsically patterned corrals in monolayer Ag5Se2 and selective molecular co-adsorption. Nano Research, 2022, 15, 6730-6735.	10.4	3
95	Role of the V2O3(0001) Defect Structure in the Adsorption of Au Adatoms. Journal of Physical Chemistry C, 2011, 115, 3404-3409.	3.1	2
96	Separation-dependence evolution of inter-particle interaction in the oriented-attachment growth of nanorods: a case of hexagonal nanocrystals. Analyst, The, 2014, 139, 3393-3397.	3.5	2
97	Direct probing of imperfection-induced electrical degradation in millimeter-scale graphene on SiO ₂ substrates. 2D Materials, 2019, 6, 045033.	4.4	2
98	Real-space observation on standing configurations of phenylacetylene on Cu (111) by scanning probe microscopy*. Chinese Physics B, 2019, 28, 066801.	1.4	2
99	Interaction of two symmetric monovacancy defects in graphene. Chinese Physics B, 2019, 28, 046801.	1.4	2
100	The evaluation of van der Waals interaction in the oriented-attachment growth of nanotubes. Materials Research Society Symposia Proceedings, 2014, 1705, 1.	0.1	0
101	Substrate tuned reconstructed polymerization of naphthalocyanine on Ag(110). Chinese Physics B, 2022, 31, 018202.	1.4	0